ANALYSIS OF THE QUALITY ASSURANCE RESULTS FROM THE INITIAL PART OF PRODUCTION OF THE ATLAS18 ITK STRIP SENSORS

È. Bach[a,*], P. Bernabeu[b], A. Bhardwaj[c], V. Cindro[d], B. Crick[c], V. Fadeyev[e], J. Fernandez-Tejero[f,g], C. Fleta[a], P. Gallus[h], K. Hara[i], S. Hirose[i], T. Ishii[i], M. Kanda[c], A. Kasum[c], J. Kroll[j], J. Kvasnicka[j], C. Lacasta[b], C.M. Mahajan[c], I. Mandić[d], M. Mikestikova[j], M. Mikuž[d], K. Nakamura[k], R.S. Orr[c], K. Sato[i], E.A. Slavikova[j], C. Solaz[b], U. Soldevila[b], P. Tuma[j], M. Ullan[a], Y. Unno[k]

[a] *Instituto de Microelectrónica de Barcelona (IMB-CNM), CSIC, Campus UAB-Bellaterra, 08193 Barcelona, Spain*

[b] *Instituto de Física Corpuscular (IFIC), CSIC, Valencia, Spain*

[c] *Department of Physics, University of Toronto, 60 Saint George St., Toronto, Ontario, Canada*

[d] *Jožef Stefan Institute, Jamova 39, Ljubljana, Slovenia*

[e] *Santa Cruz Institute for Particle Physics (SCIPP), University of California, Santa Cruz, USA*

[f] *Department of Physics, Simon Fraser University, University Drive W, Burnaby, Canada*

[g] *TRIUMF, 4004 Wesbrook Mall, Vancouver, V6T 2A3, BC, Canada*

[h] *UJP PRAHA a.s., Nad Kamínkou 1345, 156 00 Prague, Czech Republic*

[i] *Institute of Pure and Applied Sciences, University of Tsukuba, 1-1-1 Tennodai, Tsukuba, Ibaraki, Japan*

[j] *Academy of Sciences of the Czech Republic, Institute of Physics, Na Slovance 2, Prague, Czech Republic*

[k] *Institute of Particle and Nuclear Study, High Energy Accelerator Research Organization (KEK), Japan*

E-mail: eric.bach@imb-cnm.csic.es

ATL-ITK-PROC-2024-011
28 February 2024

Abstract

The production of strip sensors for the ATLAS Inner Tracker (ITk) started in 2021. Since then, a Quality Assurance (QA) program has been carried out continuously, by using specific test structures, in parallel to the Quality Control (QC) inspection of the sensors. The QA program consists of monitoring sensor-specific characteristics and the technological process variability, before and after the irradiation with gammas, neutrons, and protons. After two years, half of the full production volume has been reached and we present an analysis of the parameters measured as part of the QA process.

The main devices used for QA purposes are miniature strip sensors, monitor diodes, and the ATLAS test chip, which contains several test structures. Such devices are tested by several sites across the collaboration depending on the type of samples (non-irradiated components or irradiated with protons, neutrons, or gammas). The parameters extracted from the tests are then uploaded to a database and analyzed by Python scripts. These parameters are mainly examined through histograms and time-evolution plots to obtain parameter distributions, production trends, and meaningful parameter-to-parameter correlations. The purpose of this analysis is to identify possible deviations in the fabrication or the sensor quality, changes in the behavior of the test equipment at different test sites, or possible variability in the irradiation processes.

The conclusions extracted from the QA program have allowed test optimization, establishment of control limits for the parameters, and a better understanding of device properties and fabrication trends. In addition, any abnormal results prompt immediate

* Corresponding author

feedback to the vendor.

Keywords: Silicon strip sensors, parameter analysis

1. Introduction

The ATLAS Inner Detector is undergoing an upgrade to fulfill the major physics objectives and to meet the stringent requirements of the new HL-LHC at CERN. The resultant all-silicon detector is the Inner Tracker (ITk) detector [1], composed of both pixel and strip sensors [2]. The pixel sensors are located in the inner part of the detector, while the strip sensors are arranged surrounding the pixels in three different regions: the "barrel" region, with the sensors parallel to the beam axis, and two "endcap" regions, with sensors perpendicular to the beam axis at each side of the "barrel" region.

The strip sensors are fabricated on 6-inch, p-type, float-zone silicon wafers [3]. The sensors are fabricated in lots (batches) of 40 ± 10 wafers which are processed together. Each wafer contains one main sensor (~10x10 cm^2) at the center and four "half-moons" in the edge. Several test structures are placed in the wafer half-moons, including the test pieces used for the Quality Assurance (QA) of the production.

The Quality Control (QC) evaluation looks for defects and provides acceptance testing checks for the finished main sensors to be used in the experiment. On the other hand, the QA process aims to ensure that quality requirements are met throughout the entire fabrication process for the ATLAS ITk development. QA evaluation is based on monitoring the technology stability and keeping track of variations during the manufacturing process. This allows to predict and prevent deviations in key parameters. Furthermore, QA must ensure that the radiation hardness holds at the levels accorded during the prototyping phase. Test samples are irradiated with neutrons (Ljubljana [4], 5.1e14 n_{eq}/cm^2 and 1.6e15 n_{eq}/cm^2), protons (Birmingham, 5.1e14 n_{eq}/cm^2 [5], and CYRIC, 1.6e15 n_{eq}/cm^2 [6]) and gamma (Prague [7], 66 Mrad) to the experiment radiation targets to check the radiation hardness for each production batch. Some samples are subjected to a combined gamma+neutron (γ+n) irradiation as a substitute for the proton irradiation effect, with a dose of 66Mrad and a fluence of 1.6e15 n_{eq}/cm^2, respectively.

In terms of QA, the characteristics of any wafer are considered to be representative of its fabrication batch. For this purpose, two QA pieces are diced from every wafer: the Mini&MD8 and the Testchip&MD8. The first one is composed of a 1x1 cm^2 miniature strip sensor ("Mini"), and an 8x8 mm^2 monitoring diode ("MD8"). The second piece consists of an MD8, and the ATLAS test chip containing several test structures (bias resistors, interdigitated structures, field oxide capacitors, coupling capacitors, punch-through protection structures, and cross-bridge resistors) [8], [9]. All the parameters obtained through these devices must be within the thresholds defined by the ATLAS Collaboration.

The whole fabrication involves 4 years and about 22000 strip sensors. A delivery of sensors and QA pieces is received from the foundry and distributed for irradiation and testing every month. The produced batches have to be formally accepted by the ATLAS Collaboration within four months after delivery, therefore approval decisions are made monthly as well. At the moment of writing, the QA production has already surpassed the halfway point of the fabrication: 321 batches have been approved and only 5 have been rejected (3 of them for QA reasons). The rejected batches will be replaced later by the foundry. The QA tests details and measurement setups can be found elsewhere [10].

2. Analysis of the parameters

The irradiation and the test sites are responsible for uploading the raw test data to the ITk Production Database (DB) [11]. In the uploading process, the relevant parameters are extracted from the raw data and are also uploaded to the DB. In the data reporting process, they are selected using newly developed Python scripts which interrogate the database, filter the data and perform analysis, statistics, and representation. In this work, the parameters more relevant or with interesting features are presented using the aforementioned graphs. The objective is to track the evolution of measured parameters throughout production and maintain controlled variability.

The collected charge at 500 V is measured in Mini sensors with the ALiBaVa System [12] in the Charge Collection Efficiency (CCE) test. For neutron irradiations, this parameter is displayed as a distribution plot (Figure 1). The lowest values are very close to the minimum threshold, but pure neutron irradiations are more damaging than the particle mix expected in the ATLAS detector [13], therefore, the few lowest values are not concerning. The definition of a minimum threshold for this parameter was derived based on Signal-to-Noise (S/N) considerations and the radiation simulations and it was set at 6350 e-.

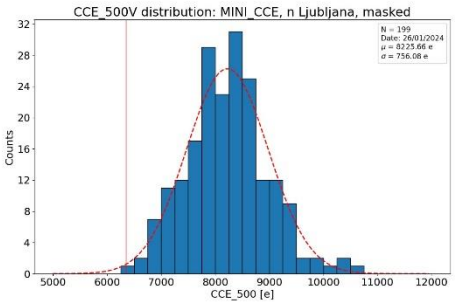

Figure 1. Distribution of the collected charge at 500 V for neutron-irradiated samples at 1.6e15 n_{eq}/cm^2.

The leakage current of MD8 diodes is measured to extract the current value at 500 V. For this parameter, γ+n irradiation (66 Mrad + 1.6e15 n_{eq}/cm^2) results are shown (Figure 2). The values measured at different test sites have been plotted using different colors. Although they remain very stable throughout the production for a given test site, small differences between test sites exist, which are assumed to be due to a temperature difference of a few degrees during the tests.

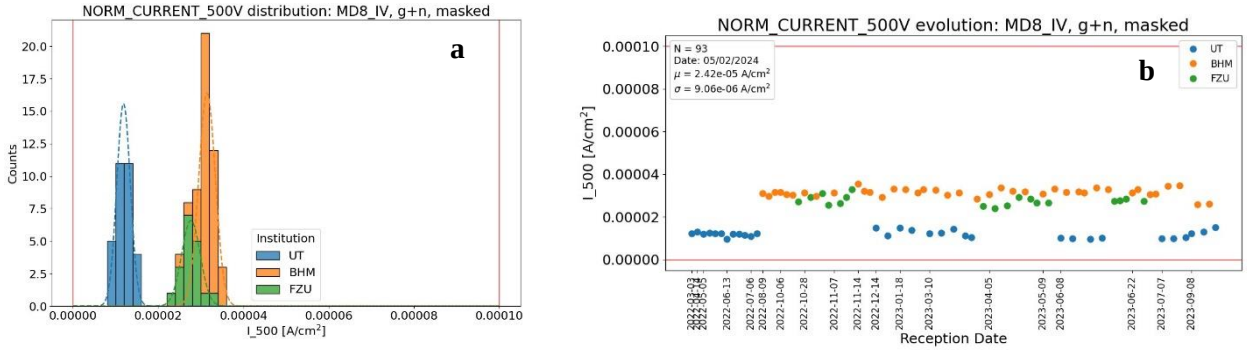

Figure 2. Distribution (a) and time-evolution (b) plots of the normalized current of the MD8 diode at 500 V measured at different test sites after γ+n irradiation.

The full depletion voltage (VFD) is extracted from the Current-Voltage characteristics (CV) of the diodes and exhibits a clear decreasing trend over time for pre-irradiated samples (Figure 3a). However, this effect appears to stabilize lately, and the observed range of values meet the specifications (> 350 V). Regarding VFD on neutron-irradiated samples (Figure 3b), some values are surpassing the maximum threshold (850 V). However, these batches have been approved on the basis of the good leakage currents from the same devices, and the good results from CCE from proton-irradiated minis. A slight increase of the average VFD post-neutrons has been observed in the latest batches without any other anomalies seen in the other QA parameters. This feature is under further investigation by the collaboration, but it does not have any significant effect on the overall quality of the sensors.

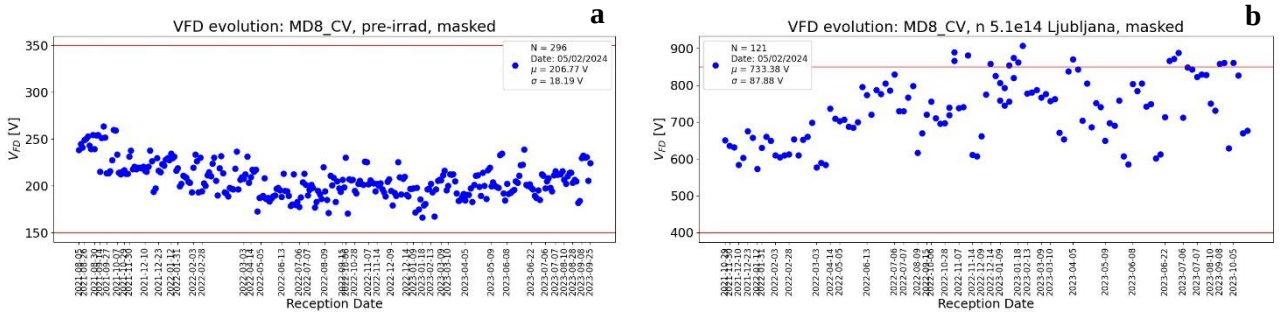

Figure 3. Representation of the VFD of the MD8 diodes over time (pre-irradiated samples).

The bias resistance is measured from separated bias resistor test structures identical to the ones in the main sensor. This parameter is plotted in Figures 4a and 4b for pre-irradiated samples and post γ+n irradiation, respectively. The measurements are temperature-corrected due to the different measurement conditions [14]. The γ+n irradiated samples show a slight increase of the resistance in comparison to the pre-irradiated ones (1.51 MΩ → 1.76 MΩ) that can be attributed to radiation effects, but both representations correspond to well-defined distributions and they satisfy the ITk requirements.

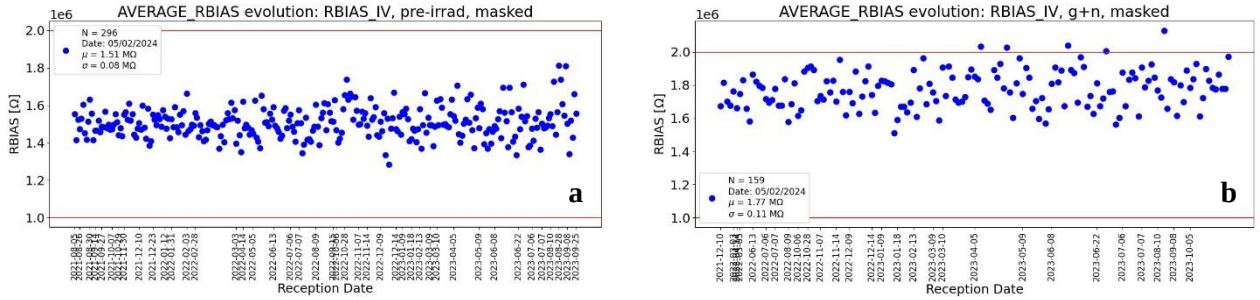

Figure 4. Time-evolution plot of the bias resistance for pre-irradiated (a) and γ+n irradiation (b).

The flat-band voltage (VFB) of the field oxide is extracted from the C-V curves at high frequency of MOS capacitors (Figure 5a). The distribution plot of VFB for this field oxide shows a high dispersion with somewhat lower average values than what is typical for gate oxides. This is probably due to an expected excess of interface traps and/or trapped charge in this type of inter-level oxides. Moreover, the distribution shows a tail towards low values, which is not critical but is being watched by the collaboration. All remaining QA parameters for these batches with lower VFB fall within the average range.

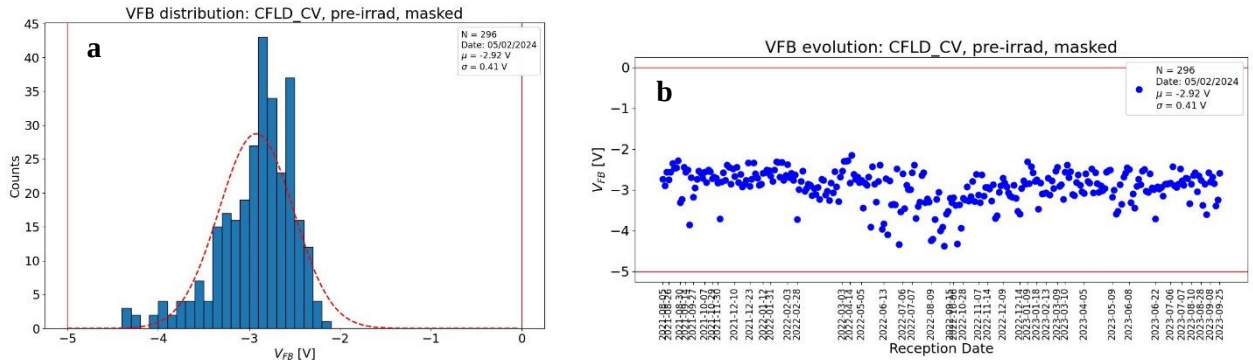

Figure 5. Distribution (a) and time-evolution (b) plots of the VFB on pre-irradiated samples.

In the MOS capacitor with a p-stop implant in the silicon underneath, the p implant affects the depletion rate of the silicon immediately underneath the oxide (Figure 6) [15]. The higher the p-implant density, the more flattened the slope of the CV curve. As seen in the figure, we defined the parameter SREF as the slope at the beginning of depletion in order to track the p-stop effect.

Three batches† have been rejected by the Collaboration due to a too-low p-stop doping density that has been detected via this test. The change in the slope due to the different p-stop implantation of one of these batches can be appreciated in Figure 7. This effect is also corroborated by Figure 8b, where the atypical values are clearly below the general trend of SREF. Furthermore, as shown below, these batches also show poor punch-through protection (PTP) performance, both on the test chips and in the main sensors. QC testings were also abnormal [16]. The Collaboration is currently doing studies with irradiated full-size sensors with low p-stop doping density to understand how this parameter affects the sensor performance.

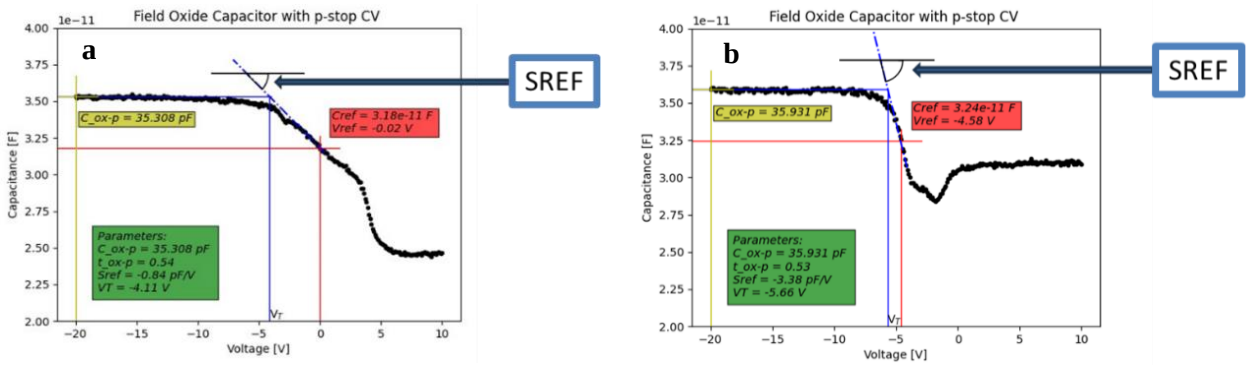

Figure 6. Examples of the extraction of the parameter SREF in a curve with a good p-stop implantation (a) and another one with low p-stop implantation (b).

† VPA37921, VPA42646, VPA46225

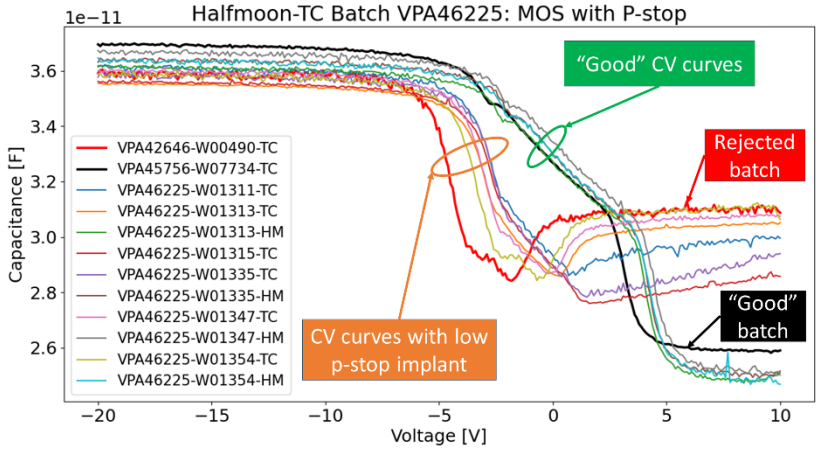

Figure 7. Extraction of the parameter SREF for "good" and rejected batches.

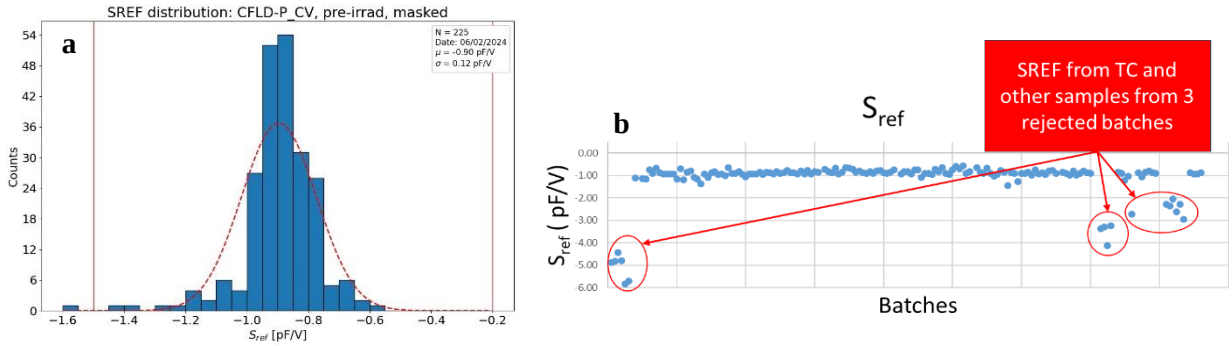

Figure 8. SREF distribution (a) and SREF representation for several batches throughout production (b). Multiple measurements performed for the rejected batches for confirmation, unlike a typical "good" batch. One SREF value lower than -1.5 V (minimum threshold), but accepted because it is close to the limit and the other QA results are correct.

The punch-through voltage (VPT) is measured with a dedicated structure. In non-irradiated test chips, this parameter is lower in the samples that also have low p-stop implantation, as can be seen in Figure 9. On the other hand, in irradiated samples with "good" p-stop implantation, the VPT remains at values that ensure the functionality of the punch-through protection after irradiation.

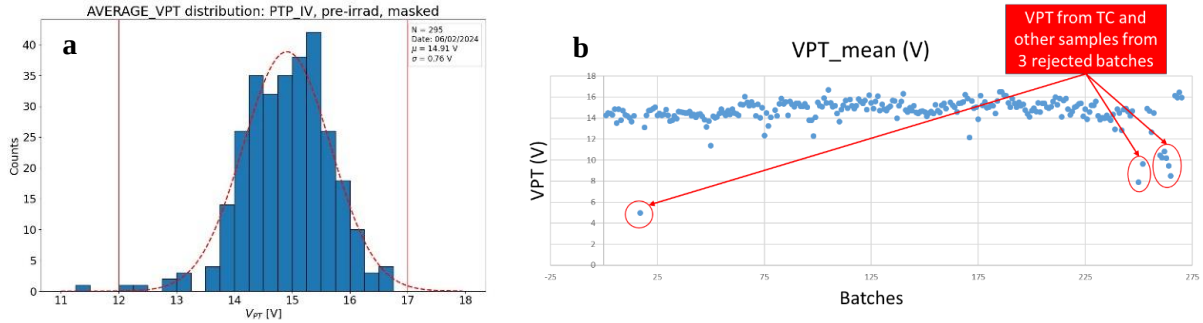

Figure 9. VPT distribution (a) and VPT representation for several batches throughout production (b) on pre-irradiated samples. One VPT value is lower than 12 V (minimum threshold), but it is accepted because it is close to the limit and the other QA results are correct.

The effective linewidth of the metal strip (WEFF-M) is a parameter measured from cross-bridge resistors (CBR) structures, only on non-irradiated samples. The distribution and time-evolution plots (Figure 10) show high dispersion due to difficult-to-measure low sheet resistance values (~0.02 Ohm/□). The mean value of WEFF-M (21 µm) is slightly lower than the nominal value (22 µm) and this discrepancy could suggest that a potential over-etching of the metal takes place during the fabrication process. This deviation is not critical as long as it remains controlled during the sensor production.

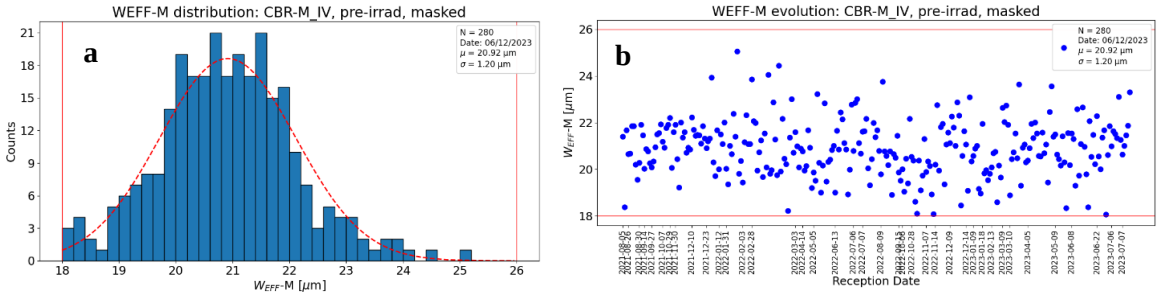

Figure 10. Distribution (a) and time-evolution (b) plots of the WEFF-M on pre-irradiated samples.

The inter-strip resistance is measured in the test chip in a specific structure designed for this purpose [8]. This parameter exhibits three clear distributions depending on the test site in γ+n-irradiated samples due to slightly different test temperatures (as also happens with the MD8 leakage currents). Figure 11a shows the distributions separately for each test site, while Figure 11b allows to see that the measurements are stable for each institute throughout production.

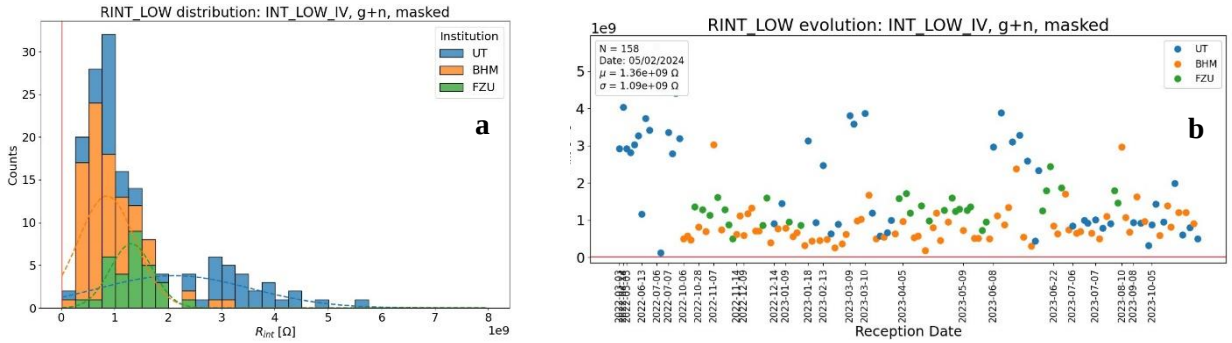

Figure 11. Distribution (a) and time-evolution (b) plots of the interstrip resistance in structures irradiated with γ+n.

Conclusions

A detailed analysis of the results of production QA tests of the ATLAS ITk strip sensor has been made. Python scripts that access the ITk database have been developed to perform this analysis and to identify fabrication trends. As a result, distribution and time-evolution plots have been obtained as tools for monitoring technological stability. This analysis has also allowed to evaluate the full QA process and the specifics of the different test sites.

After 2 years of QA evaluation, we can state that production progresses satisfactorily: 321 batches have been approved and only 3 (1%) have been rejected due to low p-stop doping.

Indeed, the 3 rejected batches confirm the need for QA tests for all batches. Both testing and irradiation have been kept fully operational. Although a few parameters have slightly exceeded the defined thresholds in some batches, most of these cases belong to the normal statistical tails in a large production. Such out-of-bounds values are watched closely to ensure the correct performance of QA, and the encountered features are well understood and stable. The production QA is progressing smoothly.

In the future, analysis must be continued by plotting correlations between parameters, re-defining and further adjusting thresholds for each parameter, and monitoring the measurement results to keep the test setups in stable operating conditions.

Acknowledgments

This work was supported by the Spanish R&D grant PID2021-126327OB-C22, funded by MCIN/ AEI/10.13039/501100011033 / FEDER, UE; the Canada Foundation for Innovation and the Natural Sciences and Engineering Research Council of Canada; the US Department of Energy, grant DE-SC0010107; the Spanish R&D grant PID2021-126327OB-C21, funded by MCIN/ AEI/10.13039/501100011033 / FEDER, UE; the European Structural and Investment Funds and the Czech Ministry of Education, Youth and Sports of the Czech Republic via projects LM2023040 CERN-CZ, LTT17018 Inter-Excellence, and FORTE - CZ.02.01.01/00/22_008/0004632.; the gamma irradiation facility UJP PRAHA a.s.; the JSPS KAKENHI Grant Number 20K22346, 23K13114; and the Slovenian Research and Innovation Agency (research core funding No. P1-0135 and project No. J1-3032). The authors would also like to thank the crew at the TRIGA reactor in Ljubljana for help with irradiations.

References

[1] L. Gonella et al., The ATLAS ITk detector system for the Phase-II LHC upgrade, Nucl. Inst. Meth. A 1045 (2023) 167597.
[2] S. Passaggio et al., The ATLAS ITk Pixel Detector: status and roadmap, CERN Document Server (CDS), 13th International Hiroshima Symposium on the Development and Application of Semiconductor Tracking Detectors, Vancouver, Ca, 6 Dec 2023, Nucl. Inst. Meth. A submitted for publication (2023), https://cds.cern.ch/record/2883326.
[3] Y. Unno et al., Specifications and pre-production of n^+-in-p large-format strip sensors fabricated in 6-inch silicon wafers, ATLAS18, for the Inner Tracker of the ATLAS Detector for High-Luminosity Large Hadron Collider, 2023 JINST 18.
[4] L. Snoj, G. Žerovnik and A. Trkov, Computational analysis of irradiation facilities at the JSI TRIGA reactor, Appl. Radiat. Isot. 70 (2012) 483.
[5] P. Allport, F. Bögelspacher, K. Bruce et al., JINST 14 (2019) P12004.
[6] Cyclotron and Radioisotope Center (CYRIC), Tohoku University, Aramaki-Aoba 6-3, Aoba-ku, Sendai-shi 980-8578, Japan.
[7] ^{60}Co irradiation facility at UJP Praha a.s. company, Prague, Czech Republic.
[8] M. Ullán et al., Quality Assurance methodology for the ATLAS Inner Tracker strip sensor production, Nucl. Inst. Meth. A 981 (2020) 164521.
[9] J. Fernandez-Tejero, Design and Optimization of Advanced Silicon Strip Detectors for High Energy Physics Experiments, PhD Thesis, Universitat Autonoma de Barcelona, 2020,

https://www.tdx.cat/handle/10803/670498#page=2.
[10] I. Kopsalis et al., Establishing the Quality Assurance programme for the strip sensor production of the ATLAS tracker upgrade including irradiation with neutrons, photons and protons to HL-LHC fluences, JINST 18 (2023) C05009
[11] V. Fadeyev et al., Monitoring Quality of ATLAS ITk Strip Sensors Through Database, PoS (Pixel2022) 058
[12] J. Bernabeu et al., ALIBAVA Silicon Microstrip Readout System for Educational Purposes, Nucl. Part. Phys. Proc. 273–275 (2016) 2563-2565
[13] K. Hara et al., Charge collection study with the ATLAS ITk prototype silicon strip sensors ATLAS17LS, Nucl. Inst. Meth. A 983 (2020) 164422
[14] V. Latoňová et al., Characterization of the polysilicon resistor in silicon strip sensors for ATLAS inner tracker as a function of temperature, pre- and post-irradiation, Nucl. Inst. Meth. A 1050 (2023) 168119.
[15] Y. Unno et al., Analysis of MOS capacitor with p layer with TCAD simulation, submitted to the special issue SI:HSTD13.
[16] P. Miyanaga et al., Analysis of the results from Quality Control tests performed on ATLAS18 Strip Sensors during on-going production, submitted to the special issue SI:HSTD13.